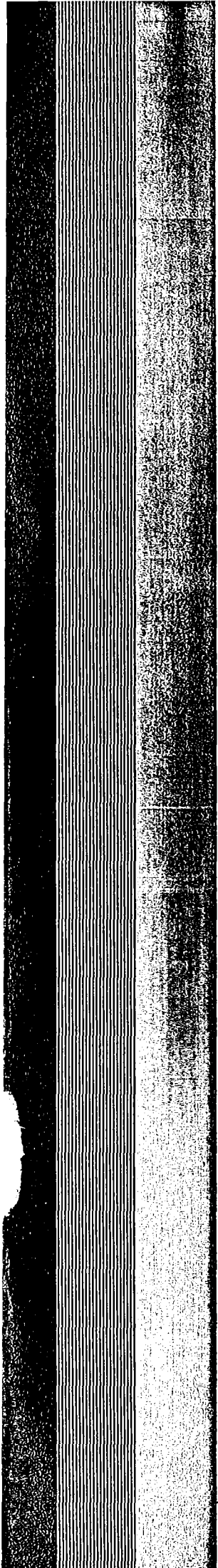# Tensile Creep Rupture at Cyclic Load Variation

M. Boček
Institut für Material- und Festkörperforschung

Kernforschungszentrum Karlsruhe

KERNFORSCHUNGSZENTRUM KARLSRUHE

Institut für Material- und Festkörperforschung

KfK - 2782

Tensile Creep Rupture at Cyclic Load Variation

von

M. Boček

Kernforschungszentrum Karlsruhe G.m.b.H., Karlsruhe

Abstract

Assuming the validity of the life fraction rule, the life time is calculated for creep rupture of material subjected to tensile cyclic stress variation. Two cases are considered: a saw - tooth stress-time profile with zero and non-zero holding period. The life times and hence the number of cycles at fracture can be predicted by means of values from the static stress-rupture diagram (n, τ_o, τ_{max}) and values characterizing the stress cycle (a, ν, t_H).

The calculations for zero holding period are compared to experiments performed on the stainless steel type: DIN 1.4970 at 700°C. Very good agreement is obtained for loading conditions leading to shorter rupture times.

Spannungszyklierung im Zugschwellbereich

Unter Annahme der Gültigkeit der Summenregel der Lebensanteile wurde die Standzeit berechnet für Materialien, die im Zug einer Wechsellastbeanspruchung unterworfen sind. Behandelt wird der Fall von Belastung mit sägezahnförmigem Spannungs-Zeit Verlauf, mit und ohne Haltezeit. Die Standzeiten und folglich auch die Bruchlastspielzahlen können vorherbestimmt werden, allein anhand der Kenngrößen statischer Zeitstanddiagramme und des Spannungs-Zeit Profils.

Die Rechnungen werden verglichen mit Ergebnissen von Experimenten am Stahl DIN 1.4970. Die Proben wurden Zug-Spannungswechseln ohne Haltezeit bei 700°C unterworfen. Die Übereinstimmung ist für kürzere Standzeiten sehr gut.
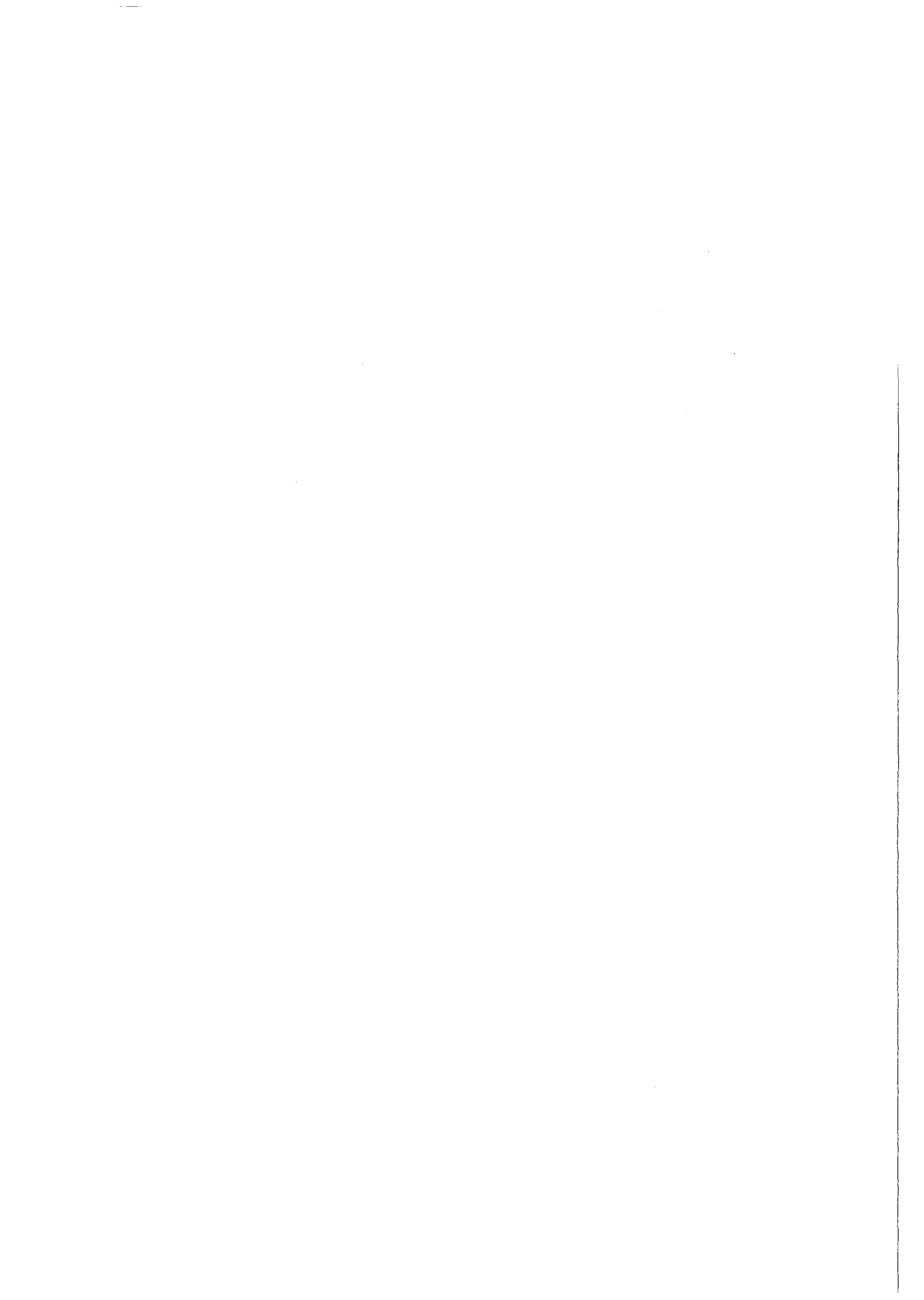
1. Introduction

The problem of predicting the life time of structures subjected to tensile creep under varying loads has been repeatedly treated. For a review see e.g. the paper of TAIRA [1]. Assuming the validity of the life fraction rule (LFR) recently the time to rupture as well as the stress and temperature at failure have been calculated by the author [2] for several ramp loading conditions. Therefore the results of ramp rupture tests can be predicted solely on the basis of iso-stress rupture experiments without any fitting procedure. As far as the fracture sensitive "structure" of the material is kept unchanged during the test, the agreement between the calculations and the experimental results turned out to be surprisingly good.
This enconraged the author to extend the model on tensile creep fracture for cyclic varying loads. As a special case a saw tooth stress-time profile with different holding periods is treated.

2. Theoretical

2.1 Saw tooth stress-time profile with zero holding period

The present case is visualized in Fig. 1. The stress-time profile is considered to be composed from two linear (time independent) stress ramps with the stress rates b_1 and $-b_1$.
For a single σ-ramp at constant temperature as far as the LFR is obeyed it holds [2]

$$\int_{\sigma_O}^{\tilde{\sigma}_B} \frac{dt}{\tau[\sigma(t)]_T} = 1 \qquad (2.1.1)$$

Where $\sigma_O, \tilde{\sigma}_B$ is the "starting" stress and the stress at failure respectively.
Inserting into Eq (2.1.1) for the life time τ from experiments [3]

$$\tau = \tau_0 \left(\frac{\sigma_O}{\sigma}\right)^n \qquad (2.1.2)$$

(where $-\frac{1}{n}$ is the solpe in the stress rupture diagram) together with

$$b = \frac{d\sigma}{dt} = const.$$

it is

$$\tilde{\sigma}_B = \left\{ \sigma_o{}^n [b\tau_o(n+1)+\sigma_o] \right\}_{T,b}^{\frac{1}{n+1}}$$

Applying in LFR to the present case it holds

$$\frac{1}{b_1} \int\limits_{\sigma_o}^{\sigma_{max}} \frac{d\sigma}{\tau(\sigma)} - \frac{1}{b_1} \int\limits_{\sigma_{max}}^{\sigma_o} \frac{d\sigma}{\tau(\sigma)} + \frac{1}{b_1} \int\limits_{\sigma_o}^{\sigma_{max}} \frac{d\sigma}{\tau(\sigma)} - \dots + \dots$$

$$= 1 \pm \frac{1}{b_1} \int\limits_{\sigma_o, \sigma_{max}}^{\sigma_f} \frac{d\sigma}{\tau(\sigma)} \tag{2.1.3}$$

or

$$M_f \int\limits_{\sigma_o}^{\sigma_{max}} \frac{d\sigma}{\tau(\sigma)} = b_1 \left\{ 1 + \frac{1}{|b_1|} \int\limits_{\sigma_o, \sigma_{max}}^{\sigma_f} \frac{d\sigma}{\tau(\sigma)} \right\} \tag{2.1.4}$$

Where M_f is the number of individual loading steps to fracture for the stress at failure σ_f it is $\sigma_o \leq \sigma_f \leq \sigma_{max}$.
It follows for the time to failure

$$^c\tau = \frac{\delta \cdot M_f}{2} + \Delta t ; \tag{2.1.5}$$

where δ is the loading period.

The term

$$\frac{1}{|b_1|} \int\limits_{\sigma_o, \sigma_{max}}^{\sigma_f} \frac{d\sigma}{\tau(\sigma)}$$

is the residuum of the serie in Eq (2.1.3). Obviously it holds for Δt in Eq (2.1.5) that

$$\Delta t = \frac{\delta}{2} \frac{\left| \int\limits_{\sigma_o, \sigma_{max}}^{\sigma_f} \frac{d\sigma}{\tau(\sigma)} \right|}{\int\limits_{\sigma_o}^{\sigma_{max}} \frac{d\sigma}{\tau(\sigma)}} \quad ; \tag{2.1.6}$$

for

$$\frac{M_f \delta}{2} \gg \Delta t \tag{2.1.7}$$

it is

$$c_\tau \doteq \frac{M_f \delta}{2} = \frac{M_f}{2\nu} = \frac{N_f}{\nu} \tag{2.1.8}$$

Where ν is the frequency and N_f the number of cycles at failure. Combining the last three equations and assuming the boundary case

$$\left| \int\limits_{\sigma_o, \sigma_{max}}^{\sigma_f} \frac{d\sigma}{\tau(\sigma)} \right| \gtrsim \int\limits_{\sigma_o}^{\sigma_{max}} \frac{d\sigma}{\tau(\sigma)} \tag{2.1.9}$$

It follows that for $\nu \gg 1$ the residuum in Eq (2.1.4) can be neglected. Thus finally we obtain

$$\int_{\sigma_o}^{\sigma_{max}} \frac{d\sigma}{\tau(\sigma)} \cdot = \frac{b_1}{N_f} \quad , \quad \text{for } \nu \gg 1 \tag{2.1.10}$$

Inserting into Eq (2.1.10) the Eq (2.1.2) together with

$$b_1 = 2 \nu (\sigma_{max} - \sigma_o) \tag{2.1.11}$$

and solving for $N_f = \frac{M_f}{2}$ it is

$$N_f = \frac{\nu \tau_o (a-1)(n+1)}{a^{(n+1)} - 1} \quad , \quad a \neq 1 \tag{2.1.12}$$

where

$$a = \frac{\sigma_{max}}{\sigma_o}$$

The time to failure follows from Eq (2.1.8) and Eq (2.1.12)

$$^c\tau = \frac{\tau_o (a-1)(n+1)}{a^{(n+1)} - 1} \quad ; \quad \text{for } \nu \gg 1 \text{ and } a \neq 1 \tag{2.1.13}$$

It is easily shown that Eq (2.1.13) obeyes the model condition

$$\lim_{a \to 1} {}^c\tau = \tau_o \tag{2.1.14}$$

Combining this with Eq (2.1.8) it follows that

$$\nu \lim_{a \to 1} {}^c\tau = \lim_{a \to 1} N_f = \nu \tau_o \tag{2.1.15}$$

In Fig. 2 several $M_f(a)$-curves are calculated using values for Zircaloy-4 [2].
The conditon for neglecting the residuum in Eq (2.1.4), that is

$$\frac{1}{|b_1|} \int\limits_{\sigma_o,\,\sigma_{max}}^{\sigma_f} \frac{d\sigma}{\tau(\sigma)} \ll 1$$

follows by combination of the above equation with the Eqs (2.1.9) (2.1.11) and the solution of the integral

$$\int\limits_{\sigma_o}^{\sigma_{max}} \frac{d\sigma}{\tau(\sigma)} \; ;$$

one obtains that

$$\nu \gg \frac{a^{(n+1)}-1}{\tau_o(a-1)(n+1)} \doteq \frac{a^{n+1}}{\tau_o(a-1)(n+1)} \tag{2.1.16}$$

2.1.1 The Equivalent Stress σ_{EQ}

We define the equivalent stress as the _static_ stress σ_{EQ} for which the corresponding life time τ equals to the life time $^c\tau$ in a stress cycling experiment.

Thus for a given a-value the condition

$$\tau = {}^c\tau$$

is obeyed for

$$\tau = \tau_o \left(\frac{\sigma_o}{\sigma_{EQ}}\right)^n$$

Combining both these equations with Eq (2.2.13) we obtain

$$\frac{\sigma_{EQ}}{\sigma_o} = \left[\frac{a^{(n+1)}-1}{(a-1)(n+1)}\right]^{1/n} \tag{2.1.1.1}$$

The condition inherent to the model is

$$\frac{\sigma_{EQ}}{\sigma_o} < a, \text{ for } a > 1$$

and

$$\lim_{a \to 1} \frac{\sigma_{EQ}}{\sigma_o} = a$$

For a particular case σ_{EQ}/σ_o is plotted as a function of a in Fig. 3; the dependency of σ_{EQ}/σ_o upon n for a=const. is shown in Fig. 4.

2.2 Saw tooth stress-time profile with finite holding period

The loading pattern for the case to be treated is shown in Fig. 5. There is one holding period per loading step. The life fraction for one cycle is

$$2\left[\frac{1}{b_1} \int_{\sigma_o}^{\sigma_{max}} \frac{d\sigma}{\tau(\sigma)} + \frac{t_H}{2} \frac{\tau_{max} + \tau_o}{\tau_o \cdot \tau_{max}}\right],$$

where t_H is the holding time and τ_{max} the life time at the constant stress σ_{max}. Assuming the validity of the LFR it is

$$M_{f,H}\left[\int_{\sigma_o}^{\sigma_{max}} \frac{d\sigma}{\tau(\sigma)} + \frac{b_1 t_H}{2} \frac{\tau_{max}+\tau_o}{\tau_{max} \cdot \tau_o}\right] = b_1(1+R) . \qquad (2.2.1)$$

$M_{f,H}$ is the number of loading steps at fracture, R denotes the residuum of the serie.

Inserting Eq (2.1.2) into Eq (2.2.1)

for R << 1 and a ≠ 1 the life time follows as

$$^c\tau_H = \frac{M_{f,H}}{2 \nu} = \frac{N_{f,H}}{\nu} = \frac{1}{\frac{a^{n+1}-1}{\tau_o(n+1)(a-1)} + t_H \nu \frac{\tau_{max}+\tau_o}{\tau_{max} \cdot \tau_o}} \qquad ; (2.2.2a)$$

if $n \gg 1$ and $\tau_o \gg \tau_{max}$ it is approximately

$$c_{\tau_H} \doteq \frac{1}{\dfrac{a^{(n+1)}}{\tau_o^{(n+1)}(a-1)} + \dfrac{t_H \nu}{\tau_{max}}} \qquad (2.2.2b)$$

As required by the model it is for $t_H = 0$

$$c_{\tau_H} = c_\tau$$

In Fig. 6 the influence of t_H upon c_{τ_H} is shown for some particular cases.

Assuming $\tau_{max} \ll \tau_o$ the condition $R \ll 1$ is obeyed if

$$\nu_H \equiv \nu \gg \frac{a^{(n+1)} - 1}{\tau_o^{(n+1)}(a-1)\left(1 - \dfrac{t_H}{\tau_{max}}\right)} \qquad (2.2.3)$$

Comparing Eq (2.2.3) with Eq (2.1.16) Eq (2.2.3) can be replaced by

$$\nu_H \gg \frac{\nu}{1 - {}^{t_H}/\tau_{max}} \qquad (2.2.4)$$

For $t_H \ll \tau_{max}$ this condition reduces to the condition defined by Eq (2.1.16) for the saw-tooth stress profile with zero holding time.

3. Experimental

In Fig. 7 the preliminary results from a serie of systematic investigations are shown for tensile stress cycling of a stainless steel of the type DIN 1.4970.

The deformation was carried out with sheet type specimens in an

"INSTRON" machine at $700^{\circ}C$ in air atmosphere. Prior to sample machining the solution annealed material was 16 % cold worked and finally annealed at $800^{\circ}C$ for 2 hours. The static stress rupture behavior of this material has been extensively examined [4]. Therefrom the following values were used for stress cycling at $T = 700^{\circ}$ C

$\tau_o = 2,2 \times 10^7$ sec (corresponds to $\sigma_o = 171$ MPA)

$n = 14$

In the experiments the lower stress limit σ_o was kept constant. The highest σ_{max}-value was 0,97 (UTS) at $700^{\circ}C$.
As one can realize from Fig. 8 the agreement between experimental values and those calculated from Eq (2.1.12) is for N_f-values below $\sim 10^3$ fairly good. The systematic deviation for higher N_f-values is probably due to a change in the microstructure of the material. For this type of steel it is reported [4] that precipitation occurs on grain boundaries when the material is subjected to long time creep.

Literature

[1] S. Taira: "Creep in Structures", Springer,
Berlin-Göttingen-Heidelberg,
1962, p. 96.

[2] M. Boček: Creep rupture at non-steady
stress and temperature loading conditions,
KfK 2699, November 1978

[3] B. Ilschner: "Hochtemperaturplastizität", Springer,
Berlin-Heidelberg-New York, 1973

[4] M. Schirra: Einfluß mechanisch-thermischer Vorbehandlung
auf das Zeitstand- und Kriechverhalten des
Strahles x 10 NiCrMoTiB 1515.
KfK 1535, Januar 1972
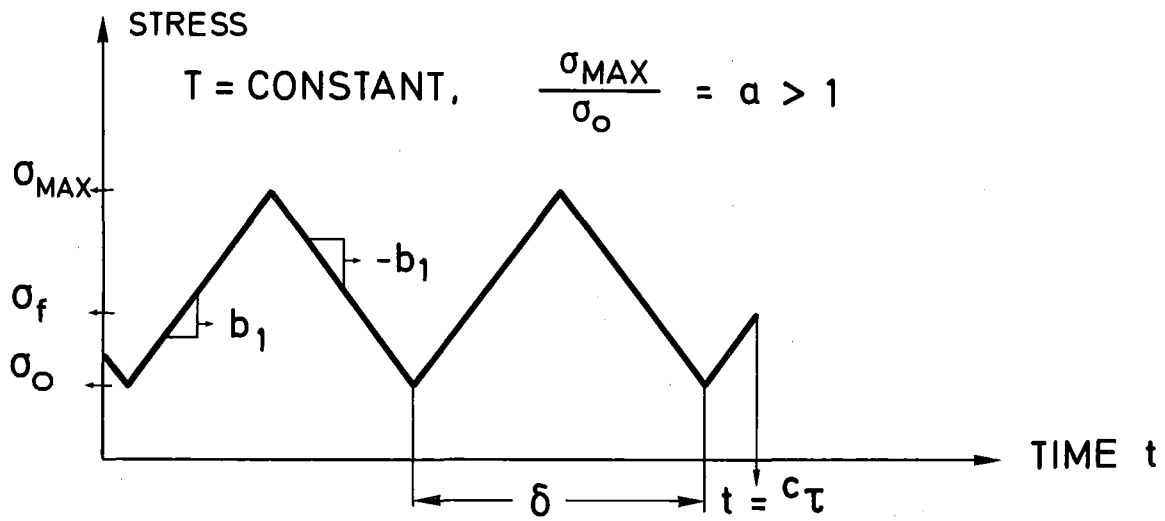
$$b_1 = 2 V \sigma_0 (a - 1) \quad \text{STRESS RATE}$$

M_f NUMBER OF HALF - CYCLES TO FRACTURE

$^c\tau$ TIME TO FRACTURE

δ PERIOD , $\frac{1}{\delta} = V$ FREQUENCY

$N_f = M_{f/2} = {}^c\tau V$ NUMBER OF CYCLES TO FRACTURE

Fig. 1 The stress-time function.
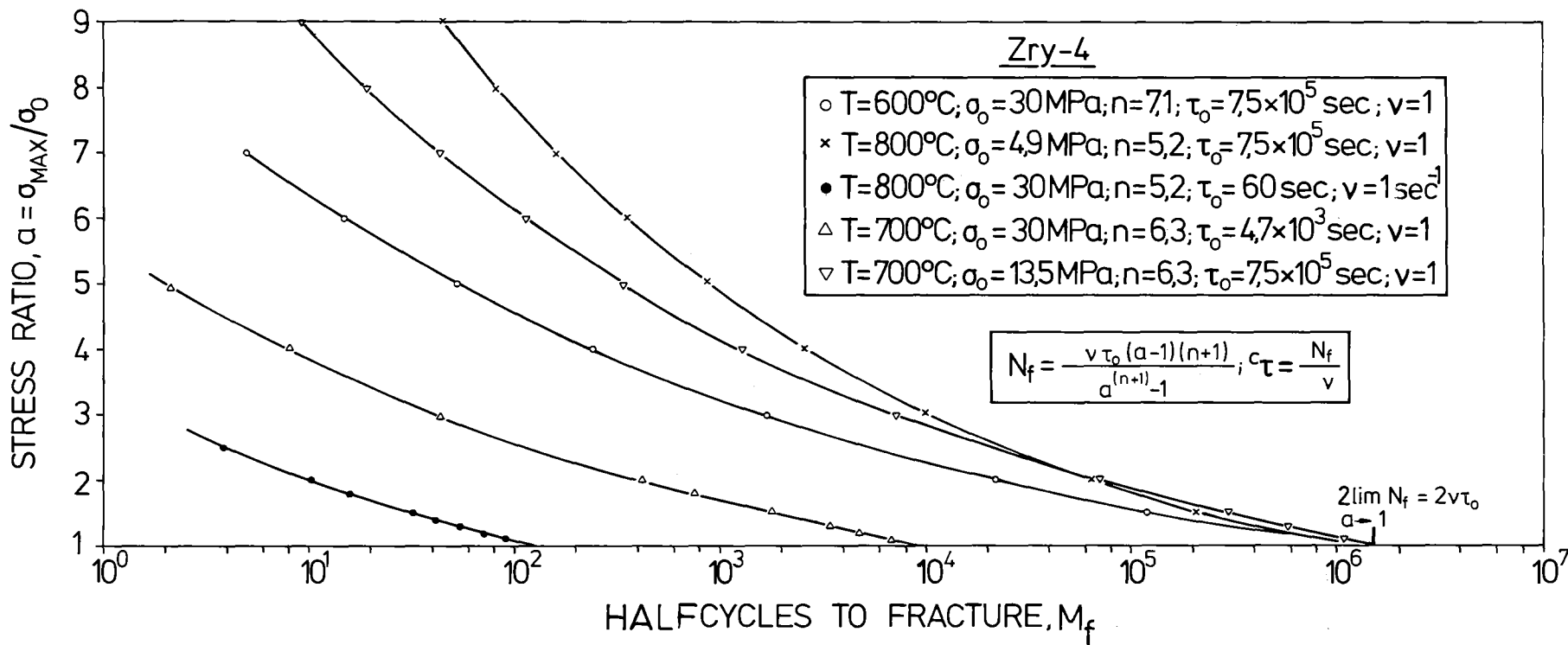
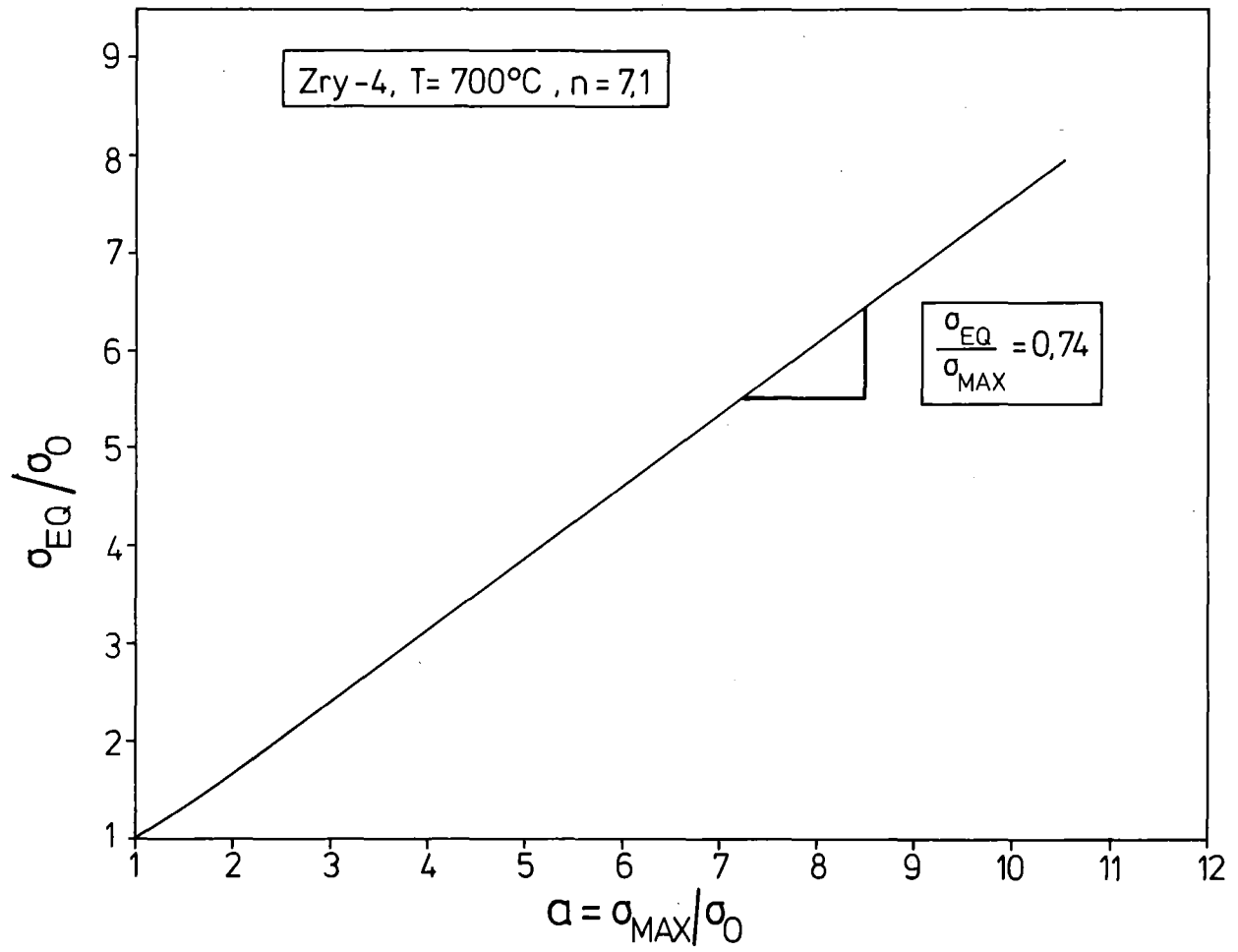Fig. 2   Number of halfcycle at failure vers. σ_{max}/σ_o.

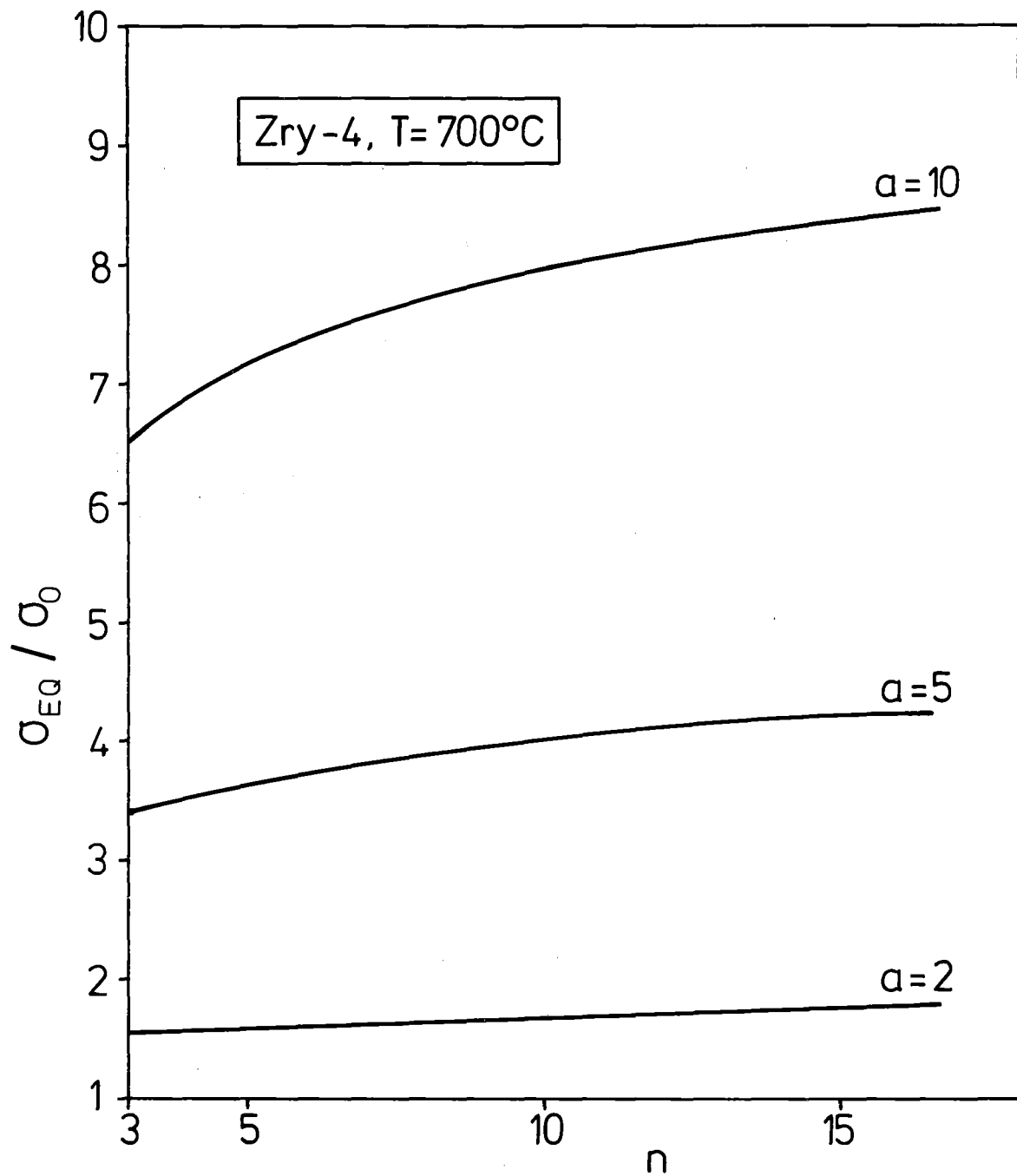Fig. 3 The dependence of σ_{EQ} upon σ_{max}.

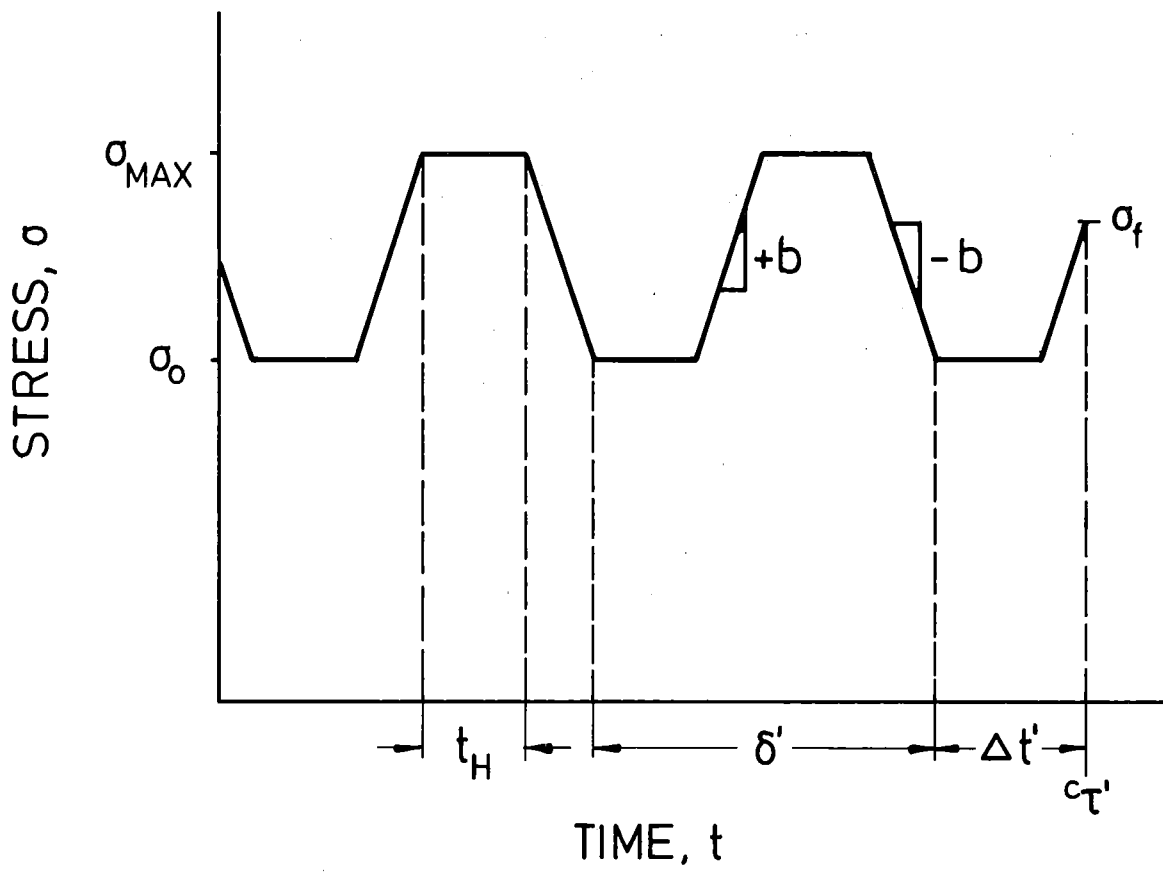Fig. 4 The stress ratio σ_{EQ}/σ_o as a function of n.
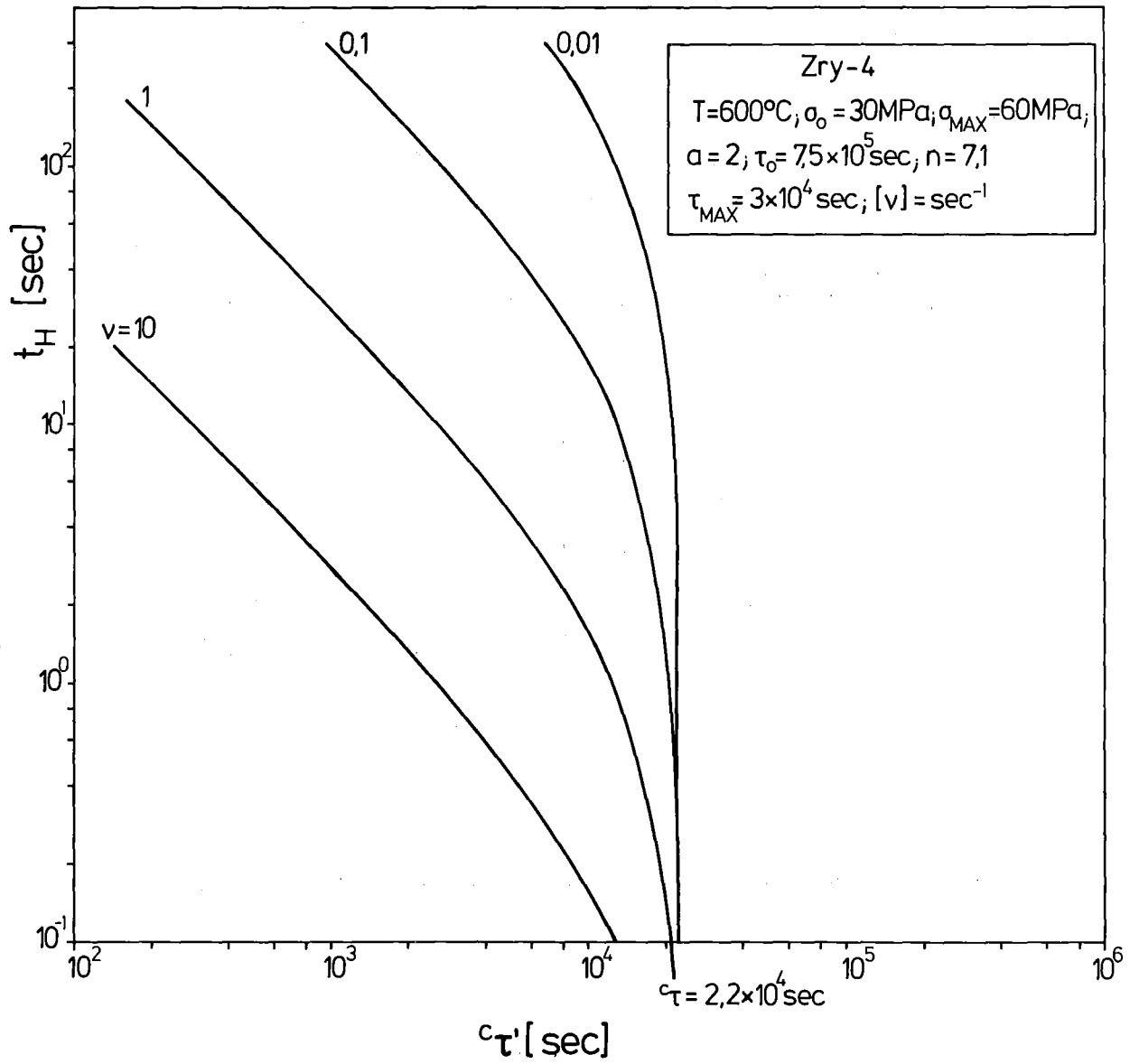
Fig. 5 The stress-time function with holding period.

Fig. 6 The dependency of the life time upon the holding time.
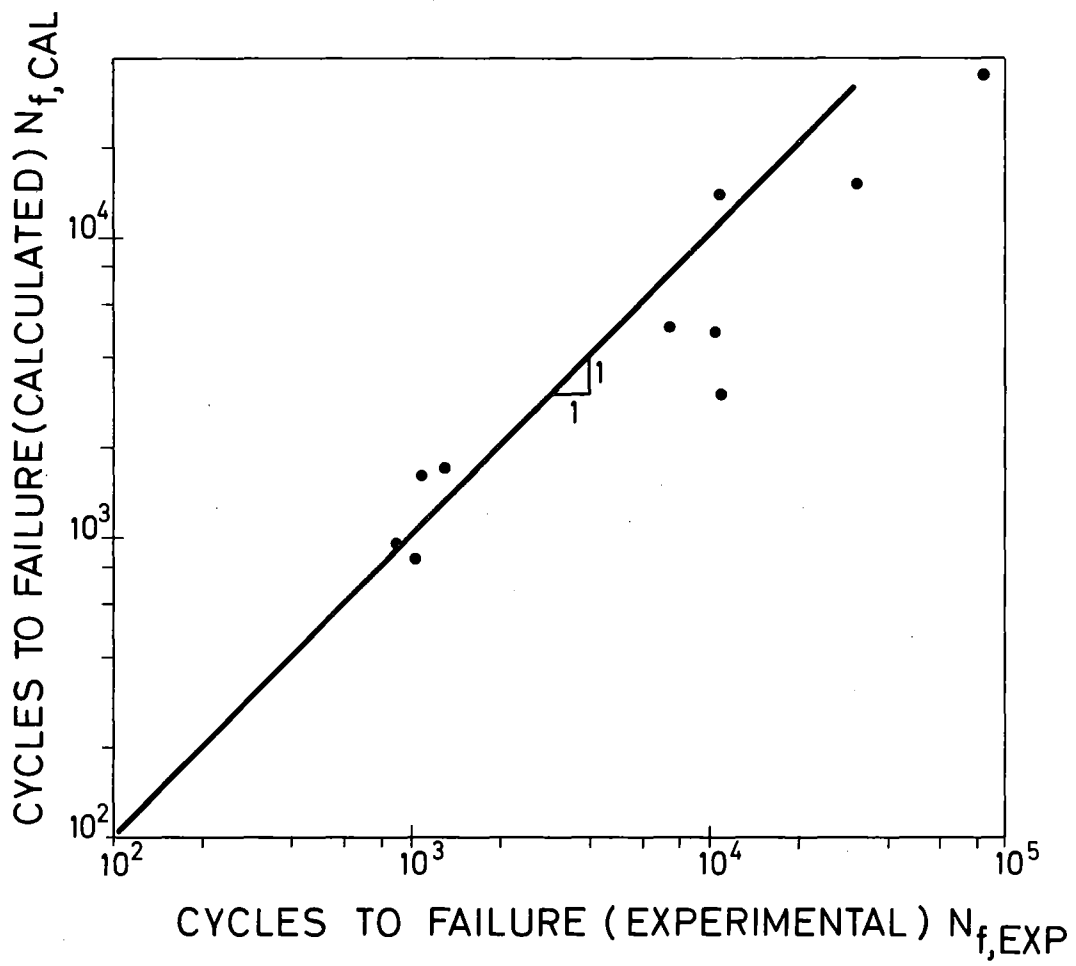
Fig. 7 An experimental $N_f(a)$-curve.

Fig. 8 Comparison of the measured N_f-values with calculated
ones.